

Phase Equilibria in the Bismuth–Oxygen System

Emmanuel Oniyama and P. G. Wahlbeck*

Department of Chemistry & National Institute for Aviation Research, Wichita State University,
Wichita, Kansas 67260-0051

Received: November 11, 1997; In Final Form: January 20, 1998

The bismuth–oxygen system was studied in the crystalline and gaseous state by means of high-temperature vaporization studies. Vaporization experiments were performed using Knudsen effusion in a high-vacuum environment and using thermogravimetric analysis with a flowing pure nitrogen environment. Oxygen was lost from samples of $\text{Bi}_2\text{O}_3(\delta)$. Compositions of residues from the vaporization experiments were determined by using thermogravimetric analysis with pure oxygen to oxidize the residues to Bi_2O_3 . The congruently effusing composition was determined to be at a composition of 1.23 O/Bi atomic ratio. The vaporization data, solid-state composition as a function of fraction of sample vaporized, could not be explained without having a new phase present in the system. The new solid phase is in accord with $\text{Bi}_{14}\text{O}_{16}$, a phase previously observed only in thin films. Pressures of the dominant gaseous species Bi and O_2 were determined by using two data: mass spectrometric intensities and the congruently effusing composition. Mass spectrometric data combined with measurements by Sidorov et al. [*High Temp. Sci.* **1980**, *12*, 175] enabled the calculation of the dissociation energy at 0 K for $\text{BiO}(\text{g})$ of 333.1 ± 3.0 kJ/mol. Pressures of Bi and O_2 were calculated using vacancy and interstitial models for the solid solution fields for the composition range 1.23–1.5 O/Bi. In addition, differential thermal analyses and quenched sample phase determinations provided data enabling construction of the Bi–O phase diagram.

Introduction

In the Bi–O system at an O_2 pressure of 1 bar, the usual phase encountered is $\text{Bi}_2\text{O}_3(\alpha)$. Different phases of Bi_2O_3 have been difficult to study because high-temperature phases quickly and easily transform to $\text{Bi}_2\text{O}_3(\alpha)$ upon sample cooling. Three additional phases for Bi_2O_3 have been reported: β , γ , and δ . The crystal structure of $\text{Bi}_2\text{O}_3(\alpha)$ is monoclinic with $a = 5.8496$ Å, $b = 8.1648$ Å, $c = 7.5101$ Å with $\beta = 112.977^\circ$.¹ $\text{Bi}_2\text{O}_3(\beta)$ is tetragonal with $a = 7.738$ Å and $c = 5.731$ Å.¹ $\text{Bi}_2\text{O}_3(\gamma)$ is body-centered cubic with $a = 10.245$ Å reported by Sillén² and $a = 10.268$ Å reported by Harwig,¹ and $\text{Bi}_2\text{O}_3(\delta)$ is face-centered cubic with $a = 5.6595$ Å.¹ The γ phase can be stabilized by impurity ions such as Al, Si, and Ge;³ the lattice parameter of the cubic lattice has been correlated with the size of the impurity ions. Harwig¹ and Medernach and Snyder⁴ both agree that $\text{Bi}_2\text{O}_3(\alpha)$ transforms to $\text{Bi}_2\text{O}_3(\delta)$ at ca. 730 °C. Upon cooling to ca. 640 °C, $\text{Bi}_2\text{O}_3(\delta)$ transforms to a metastable $\text{Bi}_2\text{O}_3(\gamma')$ phase which forms $\text{Bi}_2\text{O}_3(\alpha)$ when cooled further to ca. 500–650 °C. Harwig and Weenk⁵ have studied the structural relationships among these phases. An early study of the polymorphism of Bi_2O_3 was by Schumb and Rittner.⁶

Phase equilibria in the Bi–O system were studied previously by Isecke and Osterwald.⁷ They found at temperatures below 706 °C immiscibility between $\text{Bi}(\text{l})$ and $\text{Bi}_2\text{O}_3(\alpha)$. The solubility of oxygen in $\text{Bi}(\text{l})$ has been studied by Griffith and Mallett;⁸ the solubility limit at 750 °C is 0.20 atomic % O. Isecke and Osterwald⁷ reported that there was a phase transition in Bi_2O_3 from the α phase to the δ phase at 706 °C. At temperatures between 706 and 816 °C, a two-phase equilibrium occurred between $\text{Bi}(\text{l})$ and $\text{Bi}_2\text{O}_3(\delta)$. A eutectic line occurred at 816

°C with the three phases being $\text{Bi}(\text{l})$, the eutectic composition, and $\text{Bi}_2\text{O}_3(\delta)$. The melting point of $\text{Bi}_2\text{O}_3(\delta)$ occurs at 825 ± 3 °C.⁹

Thin films of bismuth oxides have been prepared by Zav'yalova, Imamov, and Pinsker. New phases were found in these thin films consisting of Bi_6O_8 ¹⁰ and $\text{Bi}_{14}\text{O}_{16}$.¹¹ The crystal structures for these phases were determined by using electron diffraction by Zav'yalova et al. The crystal structure of Bi_6O_8 was tetragonal with $a = 3.85$ Å and $c = 12.25$ Å, and the crystal structure of $\text{Bi}_{14}\text{O}_{16}$ was tetragonal with $a = 3.85$ Å and $c = 35.1$ Å. In another study of thin films, Schuisky and Hårsta¹² were successful in synthesizing oriented thin films of $\text{Bi}_{14}\text{O}_{16}$.

Vaporization of bismuth oxide, Bi_2O_3 , was studied by Sidorov et al.¹³ They used a Knudsen cell sample inlet system attached to a high-resolution magnetic-sector mass spectrometer. The sample in a Pt Knudsen cell was initially Bi_2O_3 . They measured intensities of several ions in the mass spectrum and concluded that the gaseous species were Bi_4O_6 , Bi_3O_4 , Bi_2O_3 , Bi_2O_2 , Bi_2O , Bi_2 , BiO , Bi , and O_2 . It was possible to calculate the vapor pressures of the observed species from the ion intensities. Sidorov et al.¹³ postulated molecular structures for the multiatom species. Another mass spectrometry experiment was performed by Kazenas, Chizhikov, Tsvetkov, and Ol'shyskii;¹⁴ they concluded that the vapor species consisted of Bi_3O_3 , Bi_4O_2 , and Bi_4O_4 . Ban and Knox¹⁵ used laser mass spectrometry and found Bi_3O_4 , in agreement with the results of Sidorov et al.,¹³ and Bi_5O_7 . Marschman and Lynch¹⁶ evaluated the bismuth oxide data and concluded that the study by Sidorov et al.¹³ was the most reliable.

Uy and Drowart¹⁷ have reported the dissociation energy of $\text{BiO}(\text{g})$ from high-temperature Knudsen cell mass spectrometry

* Corresponding author.

using isomolecular reaction data. The reaction involved BiO(g) and PbO(g). They found D_0° for BiO(g) to be 338.9 ± 5.9 kJ/mol.

Mass spectrometer studies using Knudsen cell sample inlets have been performed to study the dissociation of Bi₂(g) by Kohl, Uy, and Carlson¹⁸ and by Rovner, Drowart, and Drowart.¹⁹ In these studies, the dominant gaseous species were found to be Bi(g).

In the present study, a vaporization study of bismuth oxides has been performed using the following techniques: (1) vacuum vaporization using Knudsen effusion, (2) vaporization in a thermogravimetric analysis (TGA) apparatus with high-purity nitrogen as a carrier gas, and (3) Knudsen effusion mass spectrometry. Compositions of residues from the vaporization experiments were studied using an X-ray diffractometer and using oxidation to Bi₂O₃ in a TGA apparatus. Solid-state equilibria were studied by heating samples of Bi₂O₃ in a tube furnace with quenches in room-temperature air and quenches in liquid nitrogen. Phase transitions were determined by means of differential thermal analysis (DTA).

Experimental Part

Samples. Both Bi and Bi₂O₃ with purities better than 99.9995% were obtained from Johnson-Matthey. These samples were used in the vaporization experiments, and the thermal analyses are described below.

A sample of NaCl was obtained from Fisher Scientific Co. with purity better than 99.9%; this was used in the mass spectrometry experiments to calibrate the instrument response in order to determine vapor pressures.

Carrier gases of O₂ and N₂ with purities of 99.999% were obtained from a local gas supplier. The nitrogen was further purified by passing through an Oxiclear gas purifier, DGP-250-R2, from Labclear in Oakland, CA; this should remove remaining O₂(g) and H₂O(g) to less than 50 ppb.

Vaporization Experiments. Vaporization experiments were performed to determine the residue composition as a function of the fraction of the sample vaporized. These data are crucial for understanding the vaporization process.

A weighed sample of Bi₂O₃(α) was placed in an alumina sample holder obtained by drilling Aremco machinable ceramic, 502–1400, alumina. After the machining was accomplished, the sample holder was heated to 1000 °C. The sample holder was placed in a Pt susceptor with a Pt lid. Temperature was measured by using a type K thermocouple placed in a thermocouple well in the bottom of the sample holder. The experiments were performed under vacuum at pressures less than 1×10^{-5} Torr using two mercury vapor diffusion pumps connected in series. After the vaporization experiment was completed, the mass loss was determined by weighing the sample holder. The composition of the residue was determined by oxidation of the sample to Bi₂O₃(s) in the thermogravimetric apparatus (TGA) (to be described below) using flowing O₂(g). The mass gain of the sample determined by the TGA was used to calculate the composition of the residue.

Mass Spectrometry. A Uthe Technology, Inc. (UTI) quadrupole mass spectrometer, model 100C, was used with a high-temperature sample source. For a schematic drawing of the apparatus, see Myers and Wahlbeck.²⁰ The high-temperature source used a Knudsen cell with a removable lid and made from Aremco machinable ceramic 502–1400, alumina. The Knudsen cell was 13 mm o.d. and 7 mm i.d. with a cylindrical orifice 1 mm in diameter by 3 mm long. The Knudsen cell was heated by surrounding resistance heaters, and the temperature was read

with a type K thermocouple. Temperatures indicated by the thermocouple should be nearly correct because (1) the thermocouple junction was in direct contact with the Knudsen cell, (2) the walls of the Knudsen cell were ca. 3 mm thick giving good thermal conductivity, and (3) the surrounding radiation shields provided a more isothermal space. The mass spectrometer and Knudsen cell source were placed inside a vacuum-ion pumped system; the pressure was less than 1×10^{-6} Torr. The effusing molecules were made into a beam by water-cooled slits, and the beam was chopped with a rotating blade chopper driven by a stepper motor. The position of the chopper was read by an IR photocell. The output from the mass spectrometer was read by a data acquisition system connected to a laboratory computer. Data were acquired for a fixed mass (set on the quadrupole circuit) and the difference in signal was read with the chopper open and closed. The difference in intensity, I^+ , was used to compute vapor pressures by

$$P_i = KI_i^+ T/\sigma_i \eta_i F_i \quad (1)$$

where the subscript i refers to species i , P_i is the vapor pressure, T is the absolute temperature, σ_i is the ionization cross section, η_i is the electron multiplier efficiency, and F_i is the isotopic fraction. The ionization cross sections were the computed values by Mann.²¹ The constant K was determined by using NaCl(s) as a sample in the same Knudsen effusion cell and using the vapor pressure data of Ewing and Stern.²²

Thermal Analyses. TGA and DTA experiments were performed with DuPont system 2000 equipment. Both apparatuses are operated from a single computer and computer interface to acquire and analyze the data.

Two TGA experiments were performed. In both experiments, the samples were contained in an alumina cup placed in a fused quartz cup attached to the balance arm. Previously it was indicated that the TGA with oxygen as a carrier gas was used to oxidize residues from the vaporization experiments to determine their compositions. The second experiment was a vaporization experiment in which a sample of Bi₂O₃(s) was placed on the sample pan, and nitrogen (with low oxygen content) was used as a carrier gas. The mass loss and the rate of mass loss were used to calculate the composition of the residue and the vapor pressure of O₂(g) since the vapor pressure of Bi(g) was negligible. These data complement the vaporization data noted above.

DTA experiments were performed on Bi₂O₃(s) samples heated in alumina sample cups with O₂(g) and N₂(g) as carrier gases. With oxygen flowing, the sample composition remained at Bi₂O₃, and with nitrogen flowing, sample mixtures of Bi(l) and Bi₂O₃(s) were studied. Phase transitions were noted in these samples.

Sample Quenching. Sample mixtures of Bi(l) and Bi₂O₃(s) were heated in high-temperature alumina boats made by McDanel Refractory Porcelain Co. for a prolonged time and then quenched either in ambient air or in liquid nitrogen. The phases present in the quenched samples were determined by X-ray diffraction. Phase identification was possible using the JCPDS²³ data files.

X-ray Diffraction. X-ray powder diffraction (XRD) measurements were performed using a diffractometer manufactured by North American Phillips as model XRG-3100 with a Cu Kα X-ray source. Diffraction patterns were obtained on chart paper with this instrument.

Results

Vaporization Experiments. Two vaporization experiments were performed as described in the previous section. In both

TABLE 1: Vaporization Experiment Data

$T/^\circ\text{C}^a$	t/h	sample mass/g	fraction vaporized	residue O/Bi composition
640	0.75	0.3242	0.012	1.347
690	4.0	0.5748	0.042	1.342
640	1.0	0.3109	0.064	1.299
650	7.0	0.5994	0.071	1.290
655	3.5	0.3237	0.074	1.299
630	2.0	0.3067	0.0858	1.289
650	33.0	0.5999	0.1301	1.285
650	4.0	0.3986	0.155	1.285
650	3.33	0.2547	0.1639	1.299
655	4.5	0.2861	0.1655	1.271
650	5.5	0.4028	0.2018	1.257
620	6.75	0.1852	0.3197	1.250
640	3.0	0.3136	0.3247	1.243
650	7.0	0.1242	0.3486	1.241
650	72.0	0.5999	0.3659	1.240
650	6.5	0.1658	0.4318	1.224
650	7.0	0.3512	0.5239	1.251
650	6.25	0.1194	0.5293	1.198
655	5.0	0.3600	0.7294	1.228

^a Temperatures given in this column are indicated values. These temperature need to be corrected by ca. 100 $^\circ\text{C}$ as indicated by the melting of Bi_2O_3 .

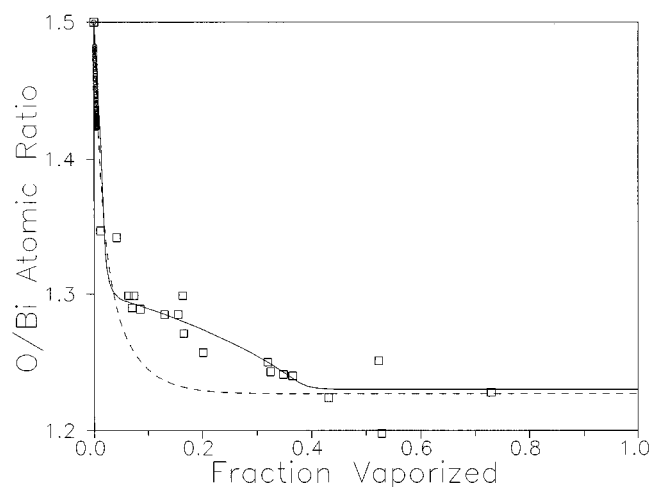


Figure 1. The fraction of the Bi_2O_3 vaporized at ca. 750 $^\circ\text{C}$. The small circular points at the left-hand side (very close to each other) were determined in TGA experiments, and the square points were from vacuum vaporization experiments. The dashed line was from a simulated data calculation using a single-condensed-phase only. The solid line was from a simulated data calculation using phase boundary estimates and vapor pressures from Figure 5.

cases the composition of the sample was determined as a function of the fraction of the sample vaporized.

Glass Vacuum System. In this case, samples of Bi_2O_3 were vaporized from an alumina crucible surrounded by an inductively heated platinum susceptor. The experiments were conducted under vacuum with a pressure less than 1×10^{-5} Torr. Mass loss data gave the amount of the sample vaporized. Reoxidation of the residue in flowing oxygen in a TGA apparatus gave the residue composition. The data from these experiments are given in Table 1 and are plotted in Figure 1.

TGA. The TGA was used for vaporization experiments in which samples of Bi_2O_3 were heated to vaporize them with nitrogen (low oxygen content) used as a carrier gas. The sample was heated to a temperature of 750 $^\circ\text{C}$ and held at that fixed temperature for 24 h. The TGA data acquisition program collected a large amount of data during the experiment. During the initial part of this experiment, the mass of the sample was changing. Data for the mass and the mass loss rate were

TABLE 2: Mass Spectrometry Results

time/min	T/K	I_{Bi^+}	$P_{\text{Bi}}/\text{Torr}$
5	991	1.095	1.161×10^{-5}
10	987	1.020	1.077×10^{-5}
15	999	5.192	5.553×10^{-5}
20	1001	5.962	6.387×10^{-5}
25	1007	7.019	7.566×10^{-5}
30	1009	5.769	6.229×10^{-5}
35	1001	8.841	9.475×10^{-5}
40	1007	10.00	10.78×10^{-5}
45	1010	10.39	11.22×10^{-5}
50	1002	9.231	9.896×10^{-5}
55	1009	8.846	9.555×10^{-5}
60	1005	10.77	11.59×10^{-5}
65	1009	12.31	13.29×10^{-5}
70	1010	8.846	9.567×10^{-5}
75	1004	6.154	6.615×10^{-5}
80	1013	8.462	9.172×10^{-5}
85	1009	7.692	8.303×10^{-5}
90	1016	9.231	10.04×10^{-5}
95	1017	8.077	8.791×10^{-5}
100	1017	8.846	9.625×10^{-5}
105	1015	9.231	10.03×10^{-5}

Calibration data using NaCl(s)			
954	55.673		1.837×10^{-3a}
959	62.404		2.075×10^{-3a}
965	71.635		2.615×10^{-3a}

^a The vapor pressures of NaCl(s) are taken from Ewing and Stern.²² These data for intensities and vapor pressures were used to calculate an average calibration constant, K , as 6.219×10^{-25} Torr/K cm^2 .

analyzed. The calculated points from the TGA experiment are shown also in Figure 1.

Mass Spectrometry. The quadrupole mass spectrometer was used with a Knudsen cell sample source. The Knudsen cell was made from alumina. A sample of Bi_2O_3 was placed inside the Knudsen cell. The vacuum during the experiments was 1×10^{-6} Torr or better.

Ions observed by the mass spectrometer were O_2^+ and Bi^+ . Ions containing multiple bismuth atoms or ions containing both bismuth and oxygen were not observed in this study. It was concluded that the vapor species were $\text{O}_2(\text{g})$ and $\text{Bi}(\text{g})$. Appearance potentials were not measured. When the sample was first heated, the pressure of $\text{O}_2(\text{g})$ was very high; a slow increase in temperature was required to prevent gaseous flooding of the vacuum pumping system.

Ion intensities were converted to vapor pressures inside the Knudsen cell using eq 1. The constant, K , of eq 1 was determined by vaporization of NaCl(s) . Data from the vaporization of NaCl(s) and Bi_2O_3 are given in Table 2 and are plotted in Figure 2. Ionization cross sections,²¹ σ , were 8.40×10^{-16} cm^2 for Bi, 3.38×10^{-16} cm^2 for Na, and 4.27×10^{-16} cm^2 for Cl; the additivity rule²⁴ was used for NaCl . Since both Na and Bi are monoisotopic, the isotopic fraction, F , is unity for both species. The multiplier gain (only the ratio is important) was given by

$$\eta_i^+ = \kappa \{1/M_i\}^{1/2} \quad (2)$$

where M_i is the molar mass of the observed ionic species.

Another sample of Bi_2O_3 was placed in the mass spectrometer Knudsen cell. It was processed through the same initial heating procedure during which the oxygen pressure was high. At the time that the Bi^+ became detectable, the heating was stopped, and the residue was analyzed using the TGA with oxygen as a carrier gas. The composition of the residue was $\text{O/Bi} = 1.324$. This is the composition for the beginning of the mass spectrometry data given in Table 2 and Figure 2. For the two-phase

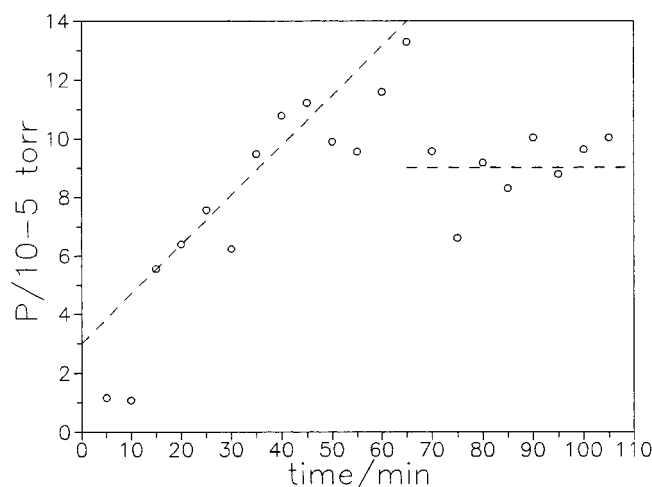


Figure 2. Pressures of Bi(g) at 740 °C as a function of time in the mass-spectrometer experiment. The composition at zero time is O/Bi of 1.324. The average pressure for the two-phase region is 9.02×10^{-5} Torr.

TABLE 3: Quenching Experiment Results

T (quench)	quench	phases
no heating		$\text{Bi}_2\text{O}_3(\alpha)$
600	air	$\text{Bi}_2\text{O}_3(\alpha)$
700	air	$\text{Bi}_2\text{O}_3(\alpha)$
800	air	$\text{Bi}_2\text{O}_3(\alpha)$
600	liq N_2	$\text{Bi}_2\text{O}_3(\alpha)$
700	liq N_2	$\text{Bi}_2\text{O}_3(\alpha), \text{Bi}_2\text{O}_3(\gamma)^a$
800	liq N_2	$\text{Bi}_2\text{O}_3(\alpha), \text{Bi}_2\text{O}_3(\gamma)^a$

^a The XRD patterns of the quenched samples showed that $\text{Bi}_2\text{O}_3(\gamma)$ was present; the high-temperature phase is actually $\text{Bi}_2\text{O}_3(\delta)$.

TABLE 4: Transition Temperatures^a from DTA Experiments

Bi–O composition % Bi	heating			cooling ^b		
	MP (Bi)	α – δ	MP (Bi_2O_3)	MP (Bi_2O_3)	γ – α^c	MP (Bi)
100	266	759			643	241
90	266	721		815		234
80	272	732	818	823		
70	267	721	811	808	601	239
60	267	733	805	811		230
50	264	720	814	807		237
40	258	730	813	811		241
30	265	743	808	808	657	
20	267	729	807	815	629	
10		723			745	
0 ^d		725			661	

^a The temperatures reported in this table are onset values. ^b In addition to the peaks indicated in the table, there was a broad endotherm which appears at ca. 785 °C in Bi_2O_3 and in samples with 60 and 70% Bi. ^c The DTA data are in agreement with the results of Harwig¹ and Medernach and Snyder⁴. On heating, α transforms to δ ; on cooling δ transforms to metastable γ which transforms to α at a lower temperature. ^d These data were acquired with flowing oxygen in the DTA apparatus.

region seen in Figure 2, the average pressure of Bi(g) for times greater than 70 min was found to be $(9.02 \pm 0.41) \times 10^{-5}$ Torr at an average temperature of 740 °C.

Quenching Experiments. Quenching experiments were performed in order to explore the phase diagram. Samples of Bi_2O_3 were used. These samples were placed in alumina boats and heated in an electric furnace at controlled temperatures in air. The samples were heated initially at 800 °C, cooled to the temperature of interest, and quenched in either ambient air or in liquid nitrogen. XRD patterns of the samples after the

quenching enabled the identification of phases present in the samples. The results of those experiments are given in Table 3.

DTA Experiments. Mixtures of Bi and Bi_2O_3 of varying compositions were ground. DTA experiments were performed on pure Bi_2O_3 in flowing oxygen (the composition should have remained close to Bi_2O_3), and experiments with the mixtures were done in flowing nitrogen. The phase transitions observed in the DTA data are given in Table 4.

The melting point of Bi(s) was observed on heating to be at 266 °C. For Bi_2O_3 on heating, the α to δ phase transition was observed at 725 °C. The transition from the δ phase on sample cooling was low in temperature and showed scatter. For samples containing between 20 and 80% Bi, the α to δ transition was observed at a slightly higher temperature of 728 °C, and the melting point was observed to be at a temperature of 811 °C.

MOPAC Calculations. Gaseous molecules have been postulated by Sidorov et al.¹³ and by Kazenas et al.¹⁴ as a result of their analyses of mass spectra. Semiempirical molecular orbital calculations have been performed using MOPAC^{25,26} and the PM3 parameters. Keywords used were “precise”, “force”, and “UHF”. For thermodynamic calculations, the rotational symmetry number was entered.

Sidorov et al.,¹³ on the basis of observed ions in the mass spectrum, proposed bismuth oxide molecules. The Sidorov molecules have stable molecular geometries according to MOPAC, whereas the Kazenas et al.¹⁴ molecular geometries did not give convergence by MOPAC. MOPAC did not use bonding information for any bismuth oxide molecule, and the enthalpies generated by MOPAC were very large. Stable molecular geometries were concluded using the geometry with the lowest $\Delta_f H^\circ$, and these geometries are given in Figure 3. MOPAC also produced vibrational frequencies for the molecular geometries given in Figure 3, and these frequencies are given in Table 5.

Discussion

Vaporization Experiments. Results from the vaporization experiments are shown in Figure 1. The data shown as points in Figure 1 are from two types of experiments: (1) vaporization in a glass vacuum system with the sample in an alumina crucible under high vacuum conditions and (2) TGA experiments with nitrogen with low oxygen content.

The data of Figure 1, Bi–O sample composition vs fraction of sample vaporized, indicated that the congruently effusing composition in the Bi–O system is at O/Bi equal to 1.230 ± 0.007 . Sidorov et al.¹³ assumed that the congruently effusing composition was at an O/Bi ratio of 1.5 corresponding to stoichiometric $\text{Bi}_2\text{O}_3(\delta)$.

Interpretation of the data of Figure 1 was accomplished by comparison of the results with calculated simulated data. The simulation used (1) the Knudsen effusion equation for transport of individual vapor species (Bi(g) and $\text{O}_2(\text{g})$), (2) the mass of the original sample, and (3) the dependence of the pressures of vapor species on composition (to be discussed later). Three possibilities occur for the compositions between 1.23 and 1.50 O/Bi atomic ratio. (1) If only a two-condensed-phase region occurs, the vapor composition would be $\text{O/Bi} = 1.23$, the present vapor composition, or 1.50 (assumed by Sidorov et al.). For the case of $\text{O/Bi} = 1.23$, residues formed from samples richer in oxygen would gain in oxygen content; this did not occur. For the case of $\text{O/Bi} = 1.50$, Bi_2O_3 would vaporize congruently; this did not occur. (2) If only a single condensed phase occurs

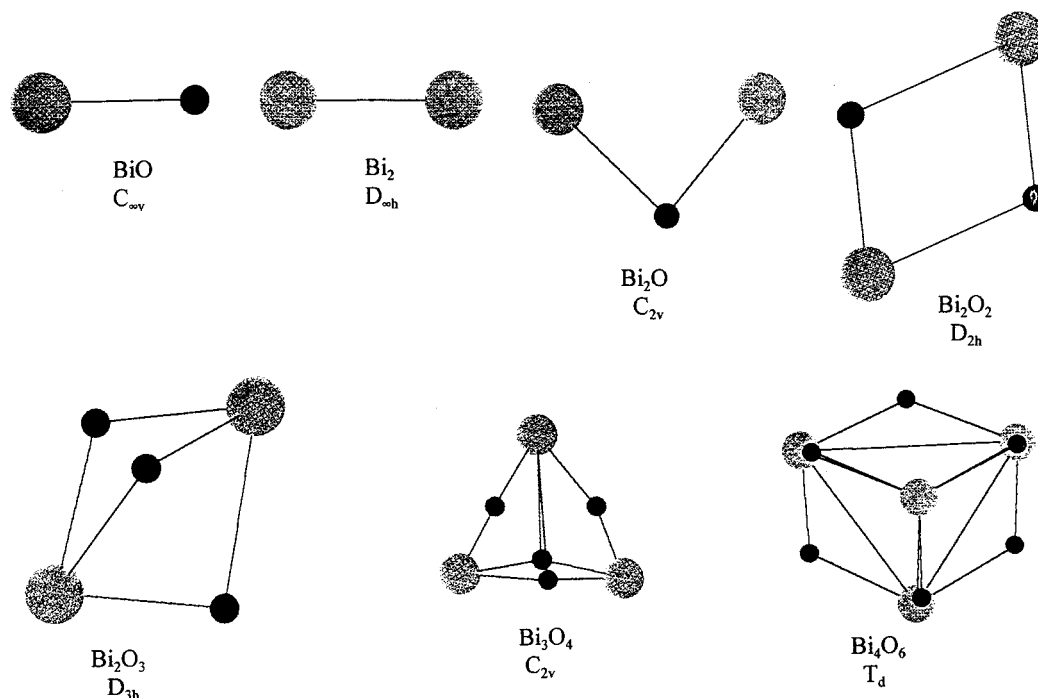


Figure 3. Stable molecular geometries as calculated by MOPAC7 using PM3 parameters.

TABLE 5: MOPAC7 Geometries and Vibrational Frequencies

molecule	geometry	vibrational ν/cm^{-1} (degeneracy)
BiO(g)	$r_o = 1.93 \text{ \AA}$	796
Bi ₂ O(g)	C_{2v} , $r(\text{Bi}-\text{O}) = 2.1 \text{ \AA}$ $\text{Bi}-\text{O}-\text{Bi} 86.6^\circ$	66 (2), 196, 956
Bi ₂ O ₂ (g)	D_{2h} , $r(\text{Bi}-\text{O}) = 2.04 \text{ \AA}$ $r(\text{Bi}-\text{Bi}) = 3.25 \text{ \AA}$ $\text{Bi}-\text{O}-\text{Bi} 105^\circ$	134, 167, 526, 587, 614, 706
Bi ₂ O ₃ (g)	D_{3h} , bipyramidal $r(\text{Bi}-\text{O}) = 2.10 \text{ \AA}$ $\text{Bi}-\text{O}-\text{Bi} 90.6^\circ$	188, 265 (2), 531 (2), 563 (2), 581, 591
Bi ₃ O ₄ (g)	C_{2v} , $r(\text{Bi}-\text{O}) = 2.06, 2.11 \text{ \AA}$ $r\text{O}-\text{O} = 2.71, 2.47 \text{ \AA}$ $\text{Bi}-\text{O}-\text{Bi} = 116.2, 93.9^\circ$	<50, 64, 82, 85, 128, 151, 183,470, 491, 504, 531, 534, 553, 691, 721
Bi ₄ O ₆ (g)	T_d , $r(\text{Bi}-\text{O}) = 2.07 \text{ \AA}$ $r(\text{Bi}-\text{Bi}) = 3.50 \text{ \AA}$ $\text{Bi}-\text{O}-\text{Bi} 106^\circ$ $\text{O}-\text{Bi}-\text{O} 106^\circ$	72 (2), 79 (3), 108 (3), 125, 170 (3), 465 (5), 489, 675 (3), 693 (3)

over the composition range, a simulated set of results, as shown in Figure 1 by a dashed line, does not agree with the experimental results. The condensed phase must be more complex. (3) A two-phase region, bounded by single-condensed-phase regions, must be present. For this case, the simulated data, even with data scatter, do fit the experimental data. (Mass spectrometric data, shown in Figure 2 and discussed later, are in agreement with case 3.)

The data of Figure 1 were compared with simulated vaporization data. The simulated data show a segment between vaporized fractions of 0.05 and 0.35 which requires a two-condensed-phase region. The phase boundaries for the two-condensed-phase region are given by the ordinates of Figure 1 at O/Bi of 1.295 ± 0.005 and 1.236 ± 0.007 . These compositions were determined by determining the compositions of Figure 1 at which the two-condensed-phase segment began and ended. The phase rule requires that there be an alternation of one- and two-condensed-phase regions. For samples with O/Bi less than 1.236, a single-phase region must exist (that phase will be concluded to be Bi₁₄O₁₆). The data plot for sample compositions with O/Bi greater than 1.35 had such a large

negative slope that it is not possible to know if another two-phase region was present.

Existence of Bi₁₄O₁₆ in Bulk. As indicated by the data analyzed from Figure 1, a single-condensed-phase region must exist with compositions of O/Bi less than 1.236. Zav'yalova et al.^{10,11} showed the existence of Bi₆O₈ and Bi₁₄O₁₆ in thin films; crystal lattice parameters were determined by electron diffraction. The stoichiometric compositions based on their crystal structures are 1.333 and 1.143, respectively. The single phase with compositions less than 1.236 is considered to be Bi₁₄O₁₆.

DTA Data. DTA data are given in Table 4. These data are in agreement with the results of Harwig¹ and those of Medernach and Snyder.⁴ The high-temperature phase was previously found to be Bi₂O₃(δ); the transition temperatures are given in Table 4. The δ phase easily transforms on cooling, and the transformation to the metastable γ phase was observed. On further cooling, the transformation of the γ phase back to the α phase was observed to occur over a temperature range.

Phase Diagram. In addition to the above phase boundary information, data are available from the DTA experiments, Table 4, and from the quenching experiments, Table 3. Additional information can be obtained from the previous phase diagram drawn by Isecke and Osterwald.⁷ A new proposed partial-phase diagram is given in Figure 4. The existence of Bi₁₄O₁₆, as discussed above, is shown on the diagram. In addition, the existence of Bi₆O₈ has been indicated tentatively because of the simple structural transformations between Bi₁₄O₁₆, Bi₆O₈, and Bi₂O₃ as oxygen content increases. These new phases were not found by Isecke and Osterwald⁷ because these phases were not stable when samples were cooled to room temperature (recall the δ transitions shown in Figure 4). The overall liquidus line of Isecke and Osterwald⁷ was approximately correct according to the proposed phase diagram shown in Figure 4.

Mass Spectrometry. Vapor effusing from an alumina Knudsen cell containing a sample which was initially Bi₂O₃ entered the ion source of a quadrupole mass spectrometer. As the sample was heated at increasing temperatures, a large amount of gas was released. This gas caused the pressure in the vacuum

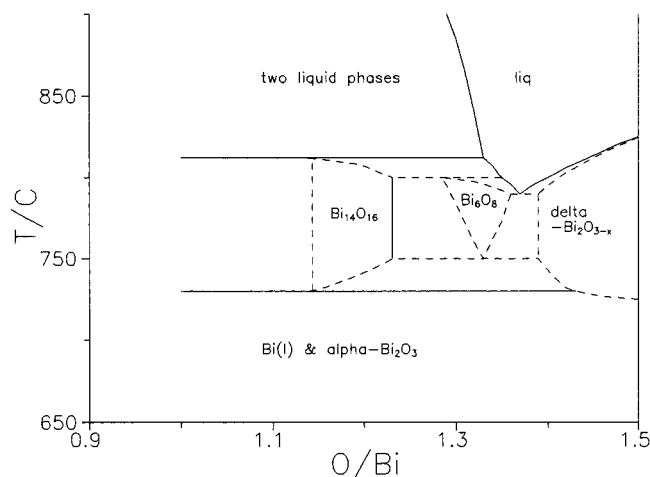


Figure 4. Proposed temperature vs composition phase diagram for the Bi–O system using data from the present study and data from Isecke and Osterwald.⁷

system to rise. After a prolonged initial heating, the vacuum system was stabilized. In one experiment, after the vacuum system was stabilized, an oxidation analysis of the sample using TGA with oxygen as a carrier gas gave a composition of O/Bi of 1.324.

The vapor species observed by the mass spectrometer were O_2^+ and Bi^+ . From these ions, the gaseous species were concluded to be $\text{O}_2(\text{g})$ and $\text{Bi}(\text{g})$. Larger molecular species were not observed in this study. The presence of species $\text{O}_2(\text{g})$ and $\text{Bi}(\text{g})$ is in agreement with the study by Sidorov et al.¹³ in which $\text{O}_2(\text{g})$ and $\text{Bi}(\text{g})$ were the most abundant species.

Ion intensities for Bi^+ were measured at an average temperature of 740 °C using a sample which had been heated so that the vacuum system was stabilized. This sample, having gone through a nearly identical heating procedure, should have had a starting composition nearly the same as that of the sample, described earlier as being 1.324. As the sample vaporized with time, the ion intensities were measured. The ion intensities were converted to $\text{Bi}(\text{g})$ pressures using eq 1 based on a pressure calibration using ion intensities and vapor pressure data of NaCl; these data are plotted in Figure 2. Sidorov et al.¹³ gave an equation for their pressures of $\text{Bi}(\text{g})$ as a function of temperature. Sidorov et al.¹³ calculated pressures from ion intensities using a different approach than that of this study. They calibrated their mass spectrometer by using the total vaporization of Bi from $\text{Bi}_2\text{O}_3(\text{s})$ and by using measured values of the equilibrium constant for two gas-phase reactions. At 740 °C, the equation from Sidorov et al.¹³ gave a pressure for $\text{Bi}(\text{g})$ of 7.7×10^{-5} Torr; the present study obtained a value of $(9.02 \pm 0.40) \times 10^{-5}$ Torr. No value for the uncertainty in the pressure of $\text{Bi}(\text{g})$ was given by Sidorov et al. These two values are in reasonable agreement, considering a reasonable uncertainty to the value by Sidorov et al. Because of this agreement for the pressures of $\text{Bi}(\text{g})$, the sample used by Sidorov et al.¹³ was probably at the congruently effusing composition of 1.23. The agreement of the present study with the results from Sidorov et al.¹³ gives added confidence in the measurements.

At the composition for congruent effusion, the composition of O/Bi is 1.23. The vapor pressure of $\text{O}_2(\text{g})$ at 740 °C would have to be given by the Knudsen equation,

$$Z_i = P_i A W / (2\pi m_i kT)^{1/2} \quad (3)$$

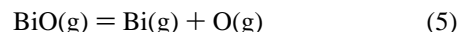
where Z_i is the rate of molecules of species i having a mass per molecule given by m_i , effusing per unit time through an orifice

with a cross-sectional area A with an orifice transmission probability W , at absolute temperature T . For the congruently effusing composition, one has

$$Z_{\text{O}_2}/Z_{\text{Bi}} = 0.615 = \{P_{\text{O}_2}/P_{\text{Bi}}\} \{M_{\text{Bi}}/M_{\text{O}_2}\}^{1/2} \quad (4)$$

At 740 °C with the bismuth pressure being 9.02×10^{-5} Torr, the oxygen pressure was calculated to be 2.17×10^{-5} Torr. Sidorov et al.¹³ had assumed that the congruently vaporizing composition was stoichiometric Bi_2O_3 which gave an oxygen pressure too large.

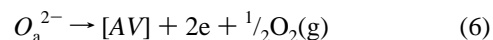
With the agreement of the vapor pressure of $\text{Bi}(\text{g})$ with that of Sidorov et al.,¹³ their value for the pressure of $\text{BiO}(\text{g})$ at 1100 K was used. Using their pressure for $\text{BiO}(\text{g})$ and the present pressures of $\text{Bi}(\text{g})$ and $\text{O}_2(\text{g})$ (calculated at 1100 K with the Sidorov temperature dependence for the pressures of $\text{Bi}(\text{g})$ and $\text{O}_2(\text{g})$), the calculation was made for the equilibrium constant at 1100 K for the dissociation reaction of $\text{BiO}(\text{g})$ (with the incorporation of the well-known equilibrium for the dissociation of $\text{O}_2(\text{g})$),



Using data from the thermochemical tables by Barin²⁷ for $\text{Bi}(\text{g})$, from JANAF²⁸ for $\text{O}(\text{g})$ and $\text{O}_2(\text{g})$, and free energy functions from Pedley and Marshall²⁹ for $\text{BiO}(\text{g})$, the dissociation energy at 0 K was calculated to be 333.1 ± 3.0 kJ/mol. This value is in agreement within the uncertainties with the value by Uy and Drowart¹⁷ of 338.9 ± 5.9 kJ/mol. Pedley and Marshall²⁹ concluded from the data of Sidorov et al.¹³ and Kazenas et al.¹⁴ that D_0° ($\text{BiO}(\text{g})$) was 333 ± 13 kJ/mol.

Defect Theory Calculations. Vapor pressures of gaseous species for a binary system depend on the temperature and the system composition. Ultimately the functional dependences of vapor pressures on composition are desired. An important feature of the phase diagram shown in Figure 4 is the existence of three solid solution regions for phases with the stoichiometric compositions given by Bi_2O_3 , Bi_6O_8 , and $\text{Bi}_{14}\text{O}_{16}$. Using solid-state defect theory, the dependences of vapor pressures on composition may be calculated. For oxygen compositions less than the stoichiometric compositions, anionic vacancies are assumed to occur. For oxygen compositions greater than the stoichiometric compositions, anionic interstitials are assumed. In the equations which follow, the concentrations of anion vacancies and oxide ion interstitials appear in the equations. These concentrations will be approximated with the ratio of either vacancies or interstitials to atoms of Bi, assuming a constant crystal volume over the single-phase composition range.

For anionic vacancies, a chemical equilibrium was considered:

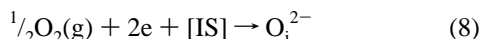


where subscript a refers to an anion site in the lattice, $[\text{AV}]$ refers to an anion vacancy in the lattice, and e refers to an electron. With $\{[\text{AV}]\}$ equal to half $\{[\text{e}]\}$, the equilibrium constant for this process yields

$$P_{\text{O}_2,r} = \text{constant } X\{[\text{AV}]\}^{-6} = \text{constant } X(c-r)^{-6} \quad (7)$$

where $\{I\}$ is used to denote the concentration of I , r is the O/Bi atomic ratio, and c is the composition of the stoichiometric phase.

For interstitial anions present in the lattice, a chemical equilibrium was considered



where subscript i refers to an interstitial site and [IS] refers to an interstitial vacancy. With $\{[\text{IS}]\}$ being a large and nearly constant value, the equilibrium constant for this process yields

$$P_{\text{O}_2,r} = \text{constant } X\{\text{O}_\text{i}^{2-}\}^2 = \text{constant } X(r - c)^2 \quad (9)$$

Equations 7 and 9 relate values for the pressure of diatomic oxygen to the composition O/Bi through the vacancy or interstitial concentrations.

Applying the Gibbs–Duhem equation³⁰ to a solution of O in Bi,

$$X_{\text{Bi}} d \ln P_{\text{Bi}} + X_{\text{O}} d \ln P_{\text{O}} = 0 \quad (10)$$

where X_i is the mole fraction of species i, the pressure of Bi(g) can be related to the composition also. It is necessary to have data for the pressure of Bi(g) from the mass spectrometer experiments and the pressure of O₂(g) determined by the congruent effusion data. For the case of oxygen anion vacancies, the Gibbs–Duhem equation integrated from the lower phase boundary of the single-phase region, z, to a general composition yields

$$P_{\text{Bi},r} = P_{\text{Bi},z} \exp[3(r - z) + 3c \ln[(c - r)/(c - z)]] \quad (11)$$

where $P_{\text{Bi},z}$ is the vapor pressure of Bi at the lower phase boundary. For the case of oxygen anion interstitials, the Gibbs–Duhem equation integrated from the upper phase boundary of the single phase, y, to a general composition yields

$$P_{\text{Bi},r} = P_{\text{Bi},y} \exp\{(y - r) - c \ln[(r - c)/(y - c)]\} \quad (12)$$

The results of these equations for the composition dependence of the pressures are shown in Figure 5. Calculations were begun at the congruently effusing composition with the measured values for P_{Bi} and P_{O_2} continuing to greater oxygen contents. If one defines the activities of Bi and O in the condensed phase by means of the equations for the vapor pressures, it is possible to calculate relative partial molal Gibbs free energies.

Vapor Species. Sidorov et al.¹³ proposed that gaseous molecules of Bi and O were Bi₄O₆, Bi₃O₄, Bi₂O₃, Bi₂O₂, Bi₂O, Bi₂, and BiO. They postulated molecular structures for these molecules. In this study, MOPAC calculations were performed, and the results are given in Table 5 with the molecular geometries given in Figure 3. The values of $\Delta_f H^\circ$ computed by MOPAC using PM3 parameters were too large; this was caused by the absence of any input data for molecules containing both Bi and O in the determination of the PM3 parameters. The structure with the smallest value of $\Delta_f H^\circ$ was considered to represent the stable molecular geometry. The assumed molecular geometries of Sidorov et al.¹³ for all his proposed molecules with the exception of Bi₃O₄ agree with the results of the MOPAC calculations. Sidorov et al.¹³ concluded that Bi₃O₄ had C_{3v} symmetry whereas MOPAC finds it to have C_{2v} symmetry.

Molecules proposed by Kazenas et al.¹⁴ with the formulas Bi₃O₃, Bi₄O₂, and Bi₄O₄ did not lead to stable MOPAC calculations. Molecules proposed by Ban and Knox¹⁵ included Bi₃O₄, also proposed by Sidorov et al.,¹³ and Bi₅O₇; MOPAC calculations on Bi₅O₇ did not lead to convergence. It is unlikely that these molecules would exist in the vapor phase.

Conclusions

Conclusions from this study are the following: (1) the congruently effusing composition for the Bi–O system is at an

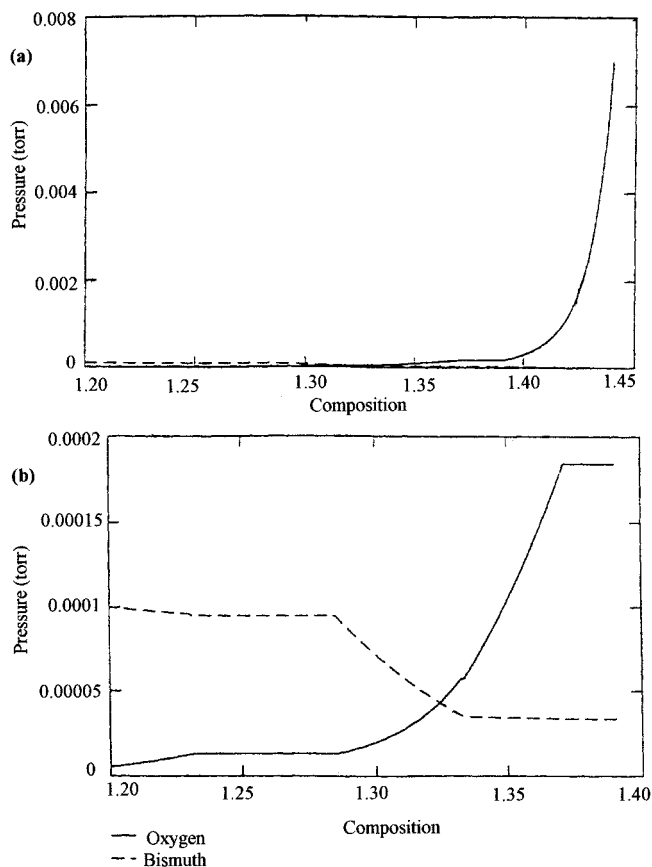


Figure 5. Calculated pressures of Bi(g) and O₂(g) at 750 °C as a function of composition using the atomic ratio O/Bi. Equations for oxide ion vacancies and interstitials were used.

O/Bi atomic ratio of 1.23 (Bi₂O₃ effuses incongruently with loss of oxygen); (2) the gaseous species from the congruently effusing composition include Bi and O₂ as the species in greatest abundance; (3) Bi₁₄O₁₆, a phase previously observed only in thin films, exists at temperatures between 730 and 812 °C; (4) the dissociation energy, D_0° , for BiO(g) was measured as 333.1 ± 3.0 kJ/mol; and (5) the measurement and calculation of vapor pressures of the dominant species as a function of composition for O/Bi atomic ratios between 1.23 and 1.5 was carried out and a proposed phase diagram was constructed.

Acknowledgment. The authors gratefully acknowledge the financial support for this research by Wichita State University. Dr. Malcolm Chase of the National Institute for Standards and Technology provided literature information. Professor Clifford Myers made valuable contributions in the review of this paper. Professor James N. Gundersen made the XRD equipment and JCPDS files available to us. The DuPont thermal analysis equipment was funded by Ametek.

References and Notes

- (1) H. A. Harwig, *Z. Anorg. Allg. Chem.* **1978**, *444*, 151.
- (2) Sillén, L. G. *Z. Kristallogr.* **1941**, *A103*, 274.
- (3) Khachani, N.; Devalette, M.; Hagenmuller, P. *Z. Anorg. Allg. Chem.* **1986**, *533*, 93.
- (4) Medernach, J. W.; Snyder, R. L. *J. Am. Cer. Soc.* **1978**, *61*, 494.
- (5) Harwig, H. A.; Weenk, J. W. *Z. Anorg. Allg. Chem.* **1978**, *444*, 167.
- (6) Schumb, W. C.; Rittner, E. S. *J. Am. Chem. Soc.* **1943**, *65*, 1055.
- (7) Isecke, B.; Osterwald, J. *Z. Phys. Chem.* **1979**, *115*, 17.
- (8) Griffith, C. B.; Mallett, M. W. *J. Am. Chem. Soc.* **1953**, *75*, 1832.
- (9) Weast, R. C. *CRC Handbook of Chemistry and Physics*, 75th, ed.; CRC Press: Boca Raton, FL, 1994.

- (10) Zav'yalova, A. A.; Imamov, R. M.; Pinsker, Z. G. *Soviet Phys. Crystallogr.* **1965**, 9, 724.
- (11) Zav'yalova, A. A.; Imamov, R. M. *Soviet Phys. — Cryst.* **1968**, 13, 37.
- (12) Schuisky, M.; Härsta, A. *Chem. Vap. Deposition* **1996**, 2, 235.
- (13) Sidorov, L. N.; Minayeva, I. I.; Zasorin, E. Z.; Sorokin, I. D.; Borshchevskiy, A. Ya. *High Temp. Sci.* **1980**, 12, 175.
- (14) Kazenas, C. K.; Chizhikov, D. M.; Tsvetkov, Y. U.; Ol'shevskii, M. V. *Dok. Akad. Nauk. SSSR* **1972**, 207, 354.
- (15) Ban, V. S.; Knox, B. E. *J. Chem. Phys.* **1970**, 52, 243.
- (16) Marschman, S. C.; Lynch, D. C. *Can. J. Chem. Eng.* **1984**, 62, 875.
- (17) Uy, O. M.; Drowart, J. *Trans. Faraday Soc.* **1969**, 65, 3221.
- (18) Kohl, F. J.; Uy, O. M.; Carlson, K. D. *J. Chem. Phys.* **1967**, 47, 2667.
- (19) Rovner, L.; Drowart, A.; Drowart, J. *Trans. Faraday Soc.* **1967**, 63, 2906.
- (20) Myers, D. L.; Wahlbeck, P. G. *J. Chem. Phys.* **1991**, 95, 5313.
- (21) Mann, J. B. *J. Chem. Phys.* **1967**, 46, 1646.
- (22) Ewing, C. T.; Stern, K. H. *J. Phys. Chem.* **1974**, 78, 1998.
- (23) JCPDS, International Center for Diffraction Data; Swarthmore: PA; 19081–2389.
- (24) Otvos, J. W.; Stevenson, D. P. *J. Am. Chem. Soc.* **1956**, 78, 546.
- (25) Stewart, J. J. P. *J. Comput. Chem.* **1989**, 10, 109, 221.
- (26) Stewart, J. J. P. *QCPE Bull.* **1983**, 3, 43.
- (27) Barin, I. *Thermochemical Data for Pure Substances*; VCH: Weim, Germany, 1989.
- (28) Chase, M. W., Jr.; Davies, C. A.; Downey, J. R., Jr.; Frurip, D. J.; McDonald, R. A.; Syverud, A. N. *JANAF Thermochemical Tables*, 3rd ed. (American Chemical Society, Washington, DC, 1985).
- (29) Pedley, J. B.; Marshall, E. M. *J. Phys. Chem. Ref. Data* **1983**, 12, 967.
- (30) Klotz, I. M.; Rosenberg, R. M. *Chemical Thermodynamics, Basic Theory and Methods*, 5th ed.; Wiley-Interscience: New York, 1994; p 258.